Title: Theta-Band Temporal Interference Stimulation of the Dorsal Anterior Cingulate Cortex Enhances Prediction Error Processing in Individuals With Food Addiction

Authors: Yatong Wen[a,b,c], Mo Wang[d,e], Xinwen Dong[a,b], Mateusz Gola[f,g], Quanying Liu[d], Yiheng Tu[a,b*], Yonghui Li[a,b*]

[a] State Key Laboratory of Cognitive Science and Mental Health, Institute of Psychology, Chinese Academy of Sciences, Beijing, China

[b] Department of Psychology, University of Chinese Academy of Sciences, Beijing, China

[c] Department of Neuroscience, Karolinska Institute, Stockholm 171 65, Sweden

[d] Department of Biomedical Engineering, Southern University of Science and Technology, Shenzhen 518055, China

[e] Department of Computer Science, University of Warwick, Coventry, United Kingdom

[f] Institute of Psychology, Polish Academy of Sciences, Warsaw, Poland

[g] Swartz Center for Computational Neuroscience, Institute for Neural Computations, University of California, San Diego, CA, USA

*Corresponding authors:

Yiheng Tu, State Key Laboratory of Cognitive Science and Mental Health, Institute of Psychology, Chinese Academy of Sciences, No.16 Lincui Road, Chaoyang District, Beijing 100101, China. Email: tuyh@psych.ac.cn

Yonghui Li, State Key Laboratory of Cognitive Science and Mental Health, Institute of Psychology, Chinese Academy of Sciences, No.16 Lincui Road, Chaoyang District, Beijing 100101, China. Email:

liyonghui@psych.ac.cn

Running title: Theta-Band tTIS of dACC and Prediction Error Processing

Keywords: temporal interference stimulation; dorsal anterior cingulate cortex; feedback-related negativity; prediction error; food addiction; electroencephalography

ABSTRACT

BACKGROUND: Food addiction is characterized by persistently elevated expectations of food reward, suggesting impairments in prediction error processing. The dorsal anterior cingulate cortex (dACC) encodes prediction errors via theta-band activity, but causal evidence in humans remains limited. Transcranial temporal interference stimulation (tTIS) offers a non-invasive approach to modulate deep cortical regions including the dACC.

METHODS: Thirty-four individuals with food addiction (15 males) were randomly assigned to active theta-band tTIS or sham stimulation. Participants completed food and monetary incentive delay tasks in a satiated state while EEG was recorded before and after stimulation. Feedback-related negativity (FRN) and stimulus preceding negativity (SPN) were examined at both mean ERP and trial-by-trial levels using behavioral and model-derived prediction errors.

RESULTS: Trial-by-trial analyses showed that tTIS selectively enhanced neural sensitivity to unfavorable food outcomes. Averaged FRN amplitudes for negative behavioral prediction errors increased after stimulation in the active group (ΔFRN = −1.91 μV, p = .038, d = 0.55), with no change in the sham group. A similar enhancement was observed for negative model-derived prediction errors (ΔFRN = −1.71 μV, p = .004, d = 0.82). At the mean ERP level, FRN during food feedback became more negative after stimulation (t_{16} = 2.75, p = .014), whereas SPN was unaffected.

CONCLUSIONS: Theta-band tTIS targeting the dACC selectively enhances neural sensitivity to prediction errors during food reward processing, highlighting temporal

interference stimulation as a tool to causally modulate deep cortical feedback-evaluation mechanisms in humans.

INTRODUCTION

Individuals with food addiction often exhibit heightened expectations of food rewards, even when satiated, potentially driven by abnormal prediction error signaling. Evidence suggests that these individuals display reduced sensitivity to this discrepancy when exposed to food-related cues (1,2). Such impairments in prediction error signaling have been associated with dysfunction in the dorsal anterior cingulate cortex (dACC) (3,4), hindering the recalibration of reward expectations and exacerbating the anticipation of food even in the absence of hunger.

The dACC encodes prediction error during reward processing primarily through theta oscillations, with its neurons continuously monitoring the process from expected outcomes to feedback, where discrepancies drive changes in neuronal activity (5). Intracranial Electroencephalogram (EEG) studies in macaques have revealed that the dACC sustains long-term error monitoring via synchronized theta rhythmic fluctuations (6). The dACC also transmits prediction error-related feedback to the dorsolateral prefrontal cortex (DLPFC) via theta rhythmic patterns, modulating phase coupling and synchrony within the DLPFC, which is essential for error processing (7). Inactivation of the dACC has been shown to reduce task-related theta activity in the prefrontal cortex, highlighting the pivotal role of theta oscillations in processing prediction error within the dACC (8).

While theta oscillations in the dACC have been linked to prediction errors, direct

evidence from theta-based interventions targeting the dACC in humans remains limited. Deep brain stimulation (DBS) of the dorsal anterior cingulate cortex has been shown to selectively modulate prediction error processing without affecting other feedback-related functions; however, this method is invasive, restricted to specific patient populations, and unable to target neural oscillations in a frequency-specific manner (9). In contrast, non-invasive neuromodulation techniques, such as transcranial alternating current stimulation (tACS), offer a promising alternative for investigating the causal roles of cortical oscillations in the brain-behavior relationships (10,11). Though rarely used to study prediction error directly, recent findings suggest that frontal cortex-targeted theta-band tACS can modulate dACC activity by reducing functional integration and hub capacity (12,13). However, these techniques are confined to superficial cortical regions and do not directly target deeper brain areas like the dACC.

Transcranial Temporal Interference Stimulation (tTIS) is a novel non-invasive neuromodulation technique that uses two high-frequency alternating currents to generate low-frequency envelopes, enabling selective stimulation of deep brain regions with targeted oscillatory patterns (14). Unlike tACS and other non-invasive methods which mainly modulate superficial cortical regions, tTIS overcomes these limitations by using high-frequency signals (>1 kHz) to target deeper brain areas. By adjusting the frequency difference between these signals, an envelope at a specific frequency can be generated, achieving a modulation effect similar to tACS (15). Recent studies have shown that tTIS can modulate subcortical activity, including in the striatum and hippocampus, across different frequency

bands (16,17), offering potential for dACC modulation with theta frequency.

In summary, the present study aimed to investigate whether theta-band tTIS modulates neural sensitivity to prediction errors during reward processing in individuals with food addiction. To address this question, we examined feedback-stage neural activity at both the average event-related potential level and the trial-by-trial level, focusing on how outcome-related discrepancies are encoded following reward feedback.

METHODS AND MATERIALS

Participants

The study was approved by the Ethics Committee of the Institute of Psychology, Chinese Academy of Sciences (No. H23113). Thirty-four right-handed participants meeting criteria for food addiction (15 males) were recruited. All participants had normal or corrected-to-normal vision and provided written informed consent in accordance with the Declaration of Helsinki.

Inclusion criteria required a Yale Food Addiction Scale (YFAS) symptom score ≥ 3 and a body mass index (BMI) ≥ 25, consistent with prior definitions of food addiction. BMI was verified by measuring height and weight prior to the experiment. Participants were randomly assigned to an tTIS group (n = 17) or a sham stimulation group (n = 17). All participants reported being in a satiated state at the time of testing, with hunger ratings below 5 on a 10-point scale, and were instructed to consume a substantial lunch before the experiment. Participants received a base payment of ¥200–¥230, with an additional performance-based bonus of up to ¥15.

Study design and procedure

The experiment consisted of three sequential phases: pretest, stimulation, and posttest. Both the pretest and posttest phases comprised 300 trials (150 food-related and 150 monetary trials), during which EEG was continuously recorded. No EEG data were collected during the stimulation phase.

Before the main experiment, participants completed a practice session and were required to achieve at least 80% accuracy to ensure adequate task comprehension. The overall experimental timeline is illustrated in Figure 1, and the structure of the incentive delay task used in both the practice and experimental phases is shown in Figure 2.

The study employed a mixed 2 × 2 design, with Group (active tTIS vs. sham stimulation) as a between-subject factor and Phase (pre- vs. post-stimulation) as a within-subject factor. Monetary trials involved generalized monetary rewards, whereas food trials depicted specific food rewards. All reward images were pre-evaluated for arousal, pleasantness, and familiarity (Supplementary Section 1).

[Insert Figure 1 here]

Incentive Delay Task

Reward processing was assessed using a modified Incentive Delay Task (IDT), adapted from Knutson et al. The task included food and monetary reward conditions. Each trial began with a cue indicating the reward type and probability (high: 80%; low: 20%), followed by a response phase in which participants indicated their reward expectation via button press. After a 2000-ms delay, feedback indicating reward or no reward was presented for 1500 ms. Inter-

trial intervals varied between 350 and 650 ms. Behavioral measures included reaction times to reward cues and reward prediction rates under high- and low-probability conditions.

[Insert Figure 2 here]

Electroencephalogram (EEG) recording and processing

Continuous scalp EEG was recorded using a 64-channel system (Neuracle NeuSen.W 64; Neuracle, Changzhou, China), with CPz as the reference and AFz as the ground. Signals were sampled at 1000 Hz in DC mode, and electrode impedances were kept below 10 kΩ. Offline data were re-referenced to the average of the bilateral mastoids (M1/M2). To dissociate neural processes related to reward anticipation and outcome evaluation, analyses focused on two established event-related potential (ERP) components: stimulus preceding negativity (SPN), indexing anticipatory processing, and feedback-related negativity (FRN), indexing feedback evaluation and the neural encoding of outcome-related discrepancies.

EEG preprocessing was performed using EEGLAB and ERPLAB toolboxes with custom MATLAB scripts. Data were filtered with a 0.1–30 Hz band-pass filter for FRN analyses and a low-pass filter at 30 Hz for SPN analyses. Epochs were segmented relative to feedback onset, and artifacts were removed using automated rejection procedures, manual inspection, and independent component analysis. SPN epochs extended from −2000 to 500 ms relative to feedback onset (baseline: −2000 to −1800 ms), capturing anticipatory activity preceding outcome presentation. FRN epochs extended from −200 to 1000 ms (baseline: −200 to 0 ms), capturing feedback-locked neural responses. ERP amplitudes were quantified from single-trial data for trial-by-trial analyses and from grand-average waveforms and scalp

topographies for visualization.

Transcranial Temporal Interference Stimulation

tTIS was delivered using an interferential neuromodulation system (Soterix Medical Inc.) targeting the left dorsal anterior cingulate cortex (dACC). Ag/AgCl electrodes (1.2 cm diameter; contact area = 1.13 cm^2) were placed according to an optimized unilateral montage (18) (Supplementary Section 2). Target coordinates (MNI: −5, 34, 30) were derived from prior neuromodulation studies (19) and verified using FSL and MNI–Talairach conversion tools (https://bioimagesuiteweb.github.io/bisweb-manual/tools/mni2tal.html). As described in Supplementary Section 2, four electrodes were used in a unilateral targeting scheme optimized for whole-brain gray matter, with electrode placements at AF3 (positive), Fz (negative), CP3 (positive), and F7 (negative).

Finite-element simulations were conducted to estimate the spatial distribution of the temporal interference envelope, which demonstrated comparable field intensity within the dACC target region (Figure 3). Stimulation consisted of two high-frequency alternating currents (2000 and 2005 Hz) generating a 5-Hz theta-band envelope. Current intensity was set to 1.6 mA (peak-to-baseline) per electrode, and stimulation lasted 20 minutes. Sham stimulation involved a 30-s ramp-up and ramp-down period without active stimulation during the remainder of the session.

[Insert Figure 3 here]

Statistical analysis

Trial-by-trial analysis of prediction error

To assess trial-wise neural sensitivity to prediction errors, linear mixed-effects (LME) models were applied to single-trial FRN amplitudes. Behavioral prediction errors were coded as −1 (worse-than-expected), 0 (expected), or +1 (better-than-expected). Prediction error, group, and phase were included as fixed effects, with subject as a random intercept. Statistical inference was based on normal approximation. All analyses were conducted in MATLAB.

Computational estimation of trial-wise prediction errors

To obtain continuous estimates of internal prediction errors, a Rescorla–Wagner reinforcement learning model was applied to trial-by-trial behavioral data. Model-derived prediction errors were computed as the difference between expected and received outcomes (see Supplementary Section 3 for model details) and entered into the same LME framework described above. In addition, subject-level FRN–prediction error slopes were estimated separately for each participant and phase as descriptive indices of individual prediction error sensitivity.

ERP and behavioral analyses

For conventional ERP and behavioral analyses, repeated-measures ANOVAs were conducted with group (active tTIS vs. sham) as a between-subject factor and phase (pre- vs. post-stimulation) as a within-subject factor. Behavioral measures included reaction times and reward prediction rates. FRN amplitudes were quantified as peak negativity within the 250–350 ms time window at FCz. For condition-level analyses and visualization, FRN waveforms were computed as difference waves (error − hit), consistent with standard definitions of FRN. SPN amplitudes were quantified as the mean voltage within the −200 to 0 ms window

preceding feedback onset. Greenhouse–Geisser corrections were applied where appropriate, with significance set at $p < .05$.

Sample size

Sample size was determined a priori using G*Power (version 3.1) for a repeated-measures analysis of variance with a within–between interaction (Group × Phase). Based on prior electroencephalography and neuromodulation studies of FRN and prediction error processing (13,20), a conservative medium effect size ($f = 0.25$) was assumed, with an alpha level of 0.05, power of 0.80, two groups, and two repeated measurements with a correlation of 0.50 ($\varepsilon = 1$). This yielded a required total sample size of 34 participants, which was therefore recruited (17 per group).

RESULTS

Demographic characteristics

A total of 34 participants with food addiction were recruited and randomly assigned to the active tTIS group (mean age = 26.29 years, SD = 5.84) or the sham stimulation group (mean age = 24.35 years, SD = 2.98). The two groups did not differ in Yale Food Addiction Scale scores, body mass index, age, education level, or household income (all $p > .05$; Table S2). All participants were tested in a satiated state, with hunger ratings below 3 and no group differences in hunger levels ($p > .05$). Mild transient sensations (e.g., headache or tingling) were more frequently reported in the active group, but no participant reported lasting discomfort or was able to correctly identify stimulation condition (Table S3).

Trial-by-trial encoding of behavioral prediction errors

To directly test whether theta-band tTIS modulates neural sensitivity to prediction errors, we first examined single-trial FRN amplitudes as a function of categorical behavioral prediction errors (PE_behavior = −1, 0, +1) using linear mixed-effects models.

FRN amplitudes scaled significantly with PE_behavior ($\beta = 1.74$, $SE = 0.30$, $z = 5.80$, $p < 10^{-8}$), such that worse-than-expected outcomes elicited more negative FRN responses. Two interaction effects indicated modulation of this encoding. A significant PE_behavior × phase interaction ($\beta = -0.89$, $SE = 0.42$, $z = -2.11$, $p = .035$) reflected a steeper FRN–PE slope after stimulation, while a significant PE_behavior × group interaction ($\beta = -1.34$, $SE = 0.43$, $z = -3.09$, $p = .002$) indicated weaker encoding in the sham group. The three-way interaction was not significant ($p > .32$).

LME-derived simple slopes were largest in the active/post condition (slope = 1.74), followed by active/pre (0.85), sham/post (0.40), and sham/pre (0.12), indicating enhanced trial-level PE sensitivity following active stimulation. Subject-level FRN–PE slopes showed a numerically similar pattern but did not reach statistical significance (active: ΔFRN= 0.81, $p = .21$; sham: ΔFRN= 0.36, $p = .45$). Averaging FRN amplitudes across trials with negative behavioral prediction errors (PE = −1) revealed a significant post-stimulation increase in FRN negativity in the active group (mean_pre = −2.51 μV, mean_post = −4.42 μV, ΔFRN = −1.91 μV, $p = .038$, $d = 0.55$), whereas the sham group showed no significant change (Figure 4).

[Insert Figure 4 here]

Trial-by-trial encoding of model-based prediction errors

We next examined whether FRN responses tracked internally estimated prediction errors derived from a Rescorla–Wagner learning model (PE_RW_behavior; Supplementary Section 3).

Single-trial FRN amplitudes scaled significantly with PE_RW_behavior ($\beta = 2.04$, $SE = 0.30$, $z = 6.74$, $p = 1.6 \times 10^{-11}$). A significant PE_RW_behavior × group interaction ($\beta = -1.25$, $SE = 0.44$, $z = -2.86$, $p = .004$) indicated weaker coupling in the sham group, while the PE_RW_behavior × phase interaction showed a trend toward stronger encoding after stimulation ($\beta = -0.76$, $SE = 0.42$, $z = -1.80$, $p = .07$). The three-way interaction was not significant ($p = .48$).

Subject-level FRN–PE_RW slopes again showed numerically larger increases in the active group but did not reach significance. In contrast, averaging FRN amplitudes across trials with negative model-derived prediction errors (PE_RW_behavior < 0) revealed a robust effect in the active group (mean_pre = −2.69 μV, mean_post = −4.40 μV, ΔFRN = −1.71 μV, $p = .004$, $d = 0.82$), with no significant change in the sham group (Figure 5).

[Insert Figure 5 here]

ERP indices of feedback and anticipation

FRN

Figure 6A shows grand-average FRN waveforms and scalp topographies elicited by food reward outcomes in the active and sham groups before and after stimulation. Across conditions, a robust FRN was observed as a fronto-central negative deflection peaking around 300 ms following feedback. Baseline FRN amplitudes did not differ between groups during

the pre-stimulation phase ($t_{32} = -0.35$, $p = .73$).

A significant main effect of phase was observed ($F_{1,32} = 6.13$, $p = .019$, $\eta_p^2 = .16$), along with a trend-level group phase interaction ($F_{1,32} = 3.86$, $p = .058$). Follow-up analyses indicated that FRN amplitudes became significantly more negative after stimulation in the active tTIS group ($t_{16} = 2.75$, $p = .014$), whereas no significant change was observed in the sham group ($t_{16} = 0.44$, $p = .67$) (Figure 8A). In contrast, FRN responses to monetary outcomes did not show significant main effects or interactions (Figure 6B; Supplementary Section 4).

[Insert Figure 6 here]

SPN

SPN waveforms and scalp distributions are shown in Figure 7. In the food IDT, baseline SPN amplitudes were comparable between groups ($t_{32} = 0.60$, $p = .55$). No significant main effects of group or phase, nor a group × phase interaction, were observed (all $p > .80$). Similar null effects were found for the monetary task (Supplementary Section 4). Quantitative SPN results are summarized in Figure 8B.

[Insert Figure 7 here]

[Insert Figure 8 here]

Behavioral data

Behavioral performance during the incentive delay task was examined to assess whether stimulation-related changes in neural prediction error encoding were accompanied by overt behavioral effects. Reaction times in the food incentive delay task showed a significant main

effect of Phase ($F_{1,32}$ = 10.73, p = .003, η_p^2 = .25), reflecting faster responses following the intervention, but no main effect of Group or Group × Phase interaction (both p > .05). Reward prediction rates did not differ as a function of Group, Phase, or their interaction for either high- or low-probability cues (all p > .05). No significant behavioral effects were observed in the monetary task (Supplementary Section 4).

DISCUSSION

To our knowledge, the present study provides the first evidence that theta-band tTIS targeting the dorsal anterior cingulate cortex (dACC) causally modulates neural sensitivity to prediction errors during reward processing in individuals with food addiction. Using a randomized, sham-controlled pre–post design, we demonstrate that theta-band tTIS selectively enhances feedback-related neural responses to unfavorable food outcomes. Crucially, this effect was most evident at the level of trial-by-trial prediction error encoding, indicating a modulation of the gain with which outcome discrepancies are represented rather than a nonspecific shift in feedback-evoked activity.

Theta-band tTIS selectively enhances feedback-stage prediction error processing

Consistent with this interpretation, at the level of average event-related potentials, theta-band tTIS was associated with a post-stimulation increase in FRN during food reward processing. FRN is widely regarded as a neural index of outcome evaluation, reflecting discrepancies between expected and actual outcomes (20,21). Notably, this modulation was specific to food rewards and was not accompanied by changes in stimulus preceding negativity (SPN), indicating that tTIS primarily affected feedback-related evaluative processes rather than

anticipatory reward signals (22).

Beyond these mean-level effects, trial-by-trial analyses revealed that FRN modulation reflected enhanced neural sensitivity to prediction errors. Single-trial FRN amplitudes scaled with both categorical behavioral prediction errors and continuous prediction errors derived from a Rescorla–Wagner model, confirming robust encoding of outcome-related information (23,24). Across both approaches, coupling between FRN amplitude and prediction error magnitude was stronger in the active stimulation group than in the sham group and numerically steeper following stimulation. These findings indicate that theta-band tTIS modulates the gain of prediction error encoding rather than merely increasing overall FRN magnitude.

dACC theta modulation as a candidate mechanism

The observed effects are consistent with the established role of the dACC in computing outcome discrepancies and guiding adaptive control through theta-band oscillatory dynamics (5,6). FRN is dominated by fronto-central theta activity and reflects the integration of outcome information with internal expectations (23,25). The selective enhancement of FRN–prediction error coupling following theta-band tTIS suggests that stimulation increased the responsivity of dACC-centered evaluative circuits to outcome discrepancies, effectively amplifying prediction error signals.

This interpretation aligns with intracranial and lesion studies showing that dACC theta oscillations regulate the salience of negative feedback and coordinate error-related signaling to lateral prefrontal regions involved in adaptive control (7,8). By modulating theta-frequency envelopes within deep cortical tissue, tTIS may bias local neuronal populations toward a state

of heightened error responsivity, strengthening the mapping between prediction error magnitude and neural response amplitude. The absence of stimulation effects on SPN further supports a dissociation between anticipatory and evaluative components of reward processing, with feedback-related theta dynamics appearing more amenable to short-term modulation (26,27). Importantly, although the stimulation protocol was designed to target theta-frequency dynamics within the dACC, the present data do not allow us to dissociate direct entrainment of local theta oscillations from indirect modulation via distributed cingulate-frontal networks. Given the dense anatomical and functional connectivity of the dACC, the observed effects likely reflect changes at the network level rather than isolated local oscillatory entrainment.

Domain specificity in food addiction

The selective modulation of FRN during food, but not monetary, reward processing is consistent with evidence that addictive behaviors are characterized by domain-specific alterations in reward-related neural responses (28,29). In eating-related disorders, food rewards preferentially engage cingulate and frontal regions compared with non–disorder-relevant rewards (30,31). Accordingly, theta-band tTIS may interact with neural circuits that are already sensitized by food-related reward learning, rather than uniformly affecting reward processing across domains. This specificity also supports the interpretability of the findings in the absence of a healthy control group, as the within-subject pre–post design with sham control directly isolates stimulation-related changes within the target population.

Implications for non-invasive modulation of deep reward-monitoring circuits

Transcranial temporal interference stimulation has been proposed as a promising approach

for modulating deep brain structures that are difficult to access using conventional non-invasive stimulation techniques (32,33). While prior work has largely relied on computational modeling or indirect behavioral outcomes, recent studies have begun to demonstrate functional effects of tTIS in humans (16,17).

By demonstrating modulation of prediction error–related neural sensitivity at the trial level, the present study extends tTIS research beyond global activation effects and highlights its potential utility for probing the causal role of deep cortical oscillatory dynamics in reinforcement learning. Importantly, the present results do not imply clinical efficacy, but rather establish a mechanistic link between theta-band tTIS and feedback-related neural encoding within the dACC.

Limitations and future directions

Several limitations should be considered. First, although the sample size was sufficient to detect medium-sized interaction effects and was further supported by trial-level linear mixed-effects analyses, it may have limited power for detecting subtle between-group differences at the level of individual slopes. However, the use of trial-level linear mixed-effects models mitigates this limitation by leveraging the full richness of the behavioral and neural data (34). Second, the study assessed only short-term effects of a single tTIS session. Future work should examine whether repeated or prolonged stimulation leads to sustained changes in prediction error sensitivity and whether such neural changes translate into measurable behavioral adaptations. Finally, although the present study focused on the dACC, reward processing involves a distributed network including the striatum and prefrontal cortex. Combining tTIS

with multimodal imaging or connectivity analyses may further elucidate how modulation of dACC theta activity influences broader reward-learning networks (35).

CONCLUSIONS

In summary, the present study demonstrates that theta-band transcranial temporal interference stimulation targeting the dACC modulates neural sensitivity to prediction errors during food reward processing in individuals with food addiction. By selectively altering trial-by-trial coupling between feedback-related neural activity and prediction error signals, tTIS provides a novel non-invasive tool for probing the neural mechanisms underlying reward learning and feedback evaluation in humans.

ACKNOWLEDGMENTS AND DISCLOSURES

This work was supported by the Chinese National Programs for Brain Science and Brain-like Intelligence Technology (Grant No. 2021ZD0202104) and the International Cooperation and Exchange Program of the National Natural Science Foundation of China (Grant No. 32161133004).

Y.T.W. had full access to all study data and takes responsibility for data integrity and analysis accuracy. Y.T.W. is the first author and contributed to study conception and design, data acquisition and analysis, and manuscript drafting. Y.H.L. and Y.H.T. obtained funding and provided supervision and critical revision of the manuscript. M.W. contributed to brain region modeling and stimulation methodology. Q.Y.L. provided methodological support and contributed to interpretation of the results. X.W.D. and M.G. contributed to interpretation of findings and critical revision of the manuscript. All authors approved the final manuscript and

agree to be accountable for all aspects of the work.

REFERENCES

1. Wen Y, Zeng Y, Zhou X, Gola M, Dong X, Li Y (2026): Satiety modulates reward processing in food addiction: Evidence from event-related potentials. *Appetite* 219: 108395.

2. Reiter AMF, Heinze H-J, Schlagenhauf F, Deserno L (2017): Impaired Flexible Reward-Based Decision-Making in Binge Eating Disorder: Evidence from Computational Modeling and Functional Neuroimaging. *Neuropsychopharmacology* 42: 628–637.

3. Fitzgerald KD, Welsh RC, Gehring WJ, Abelson JL, Himle JA, Liberzon I, Taylor SF (2005): Error-related hyperactivity of the anterior cingulate cortex in obsessive-compulsive disorder. *Biological Psychiatry* 57: 287–294.

4. Lei W, Liu K, Chen G, Tolomeo S, Liu C, Peng Z, *et al.* (2020): Blunted reward prediction error signals in internet gaming disorder. *Psychol Med* 1–10.

5. Warren CM, Hyman JM, Seamans JK, Holroyd CB (2015): Feedback-related negativity observed in rodent anterior cingulate cortex. *Journal of Physiology-Paris* 109: 87–94.

6. Womelsdorf T, Johnston K, Vinck M, Everling S (2010): Theta-activity in anterior cingulate cortex predicts task rules and their adjustments following errors. *Proc Natl Acad Sci USA* 107: 5248–5253.

7. Smith EH, Horga G, Yates MJ, Mikell CB, Banks GP, Pathak YJ, *et al.* (2019): Widespread temporal coding of cognitive control in the human prefrontal cortex. *Nat Neurosci* 22: 1883–1891.

8. Ma L, Chan JL, Johnston K, Lomber SG, Everling S (2019): Macaque anterior cingulate

cortex deactivation impairs performance and alters lateral prefrontal oscillatory activities in a rule-switching task ((E. Procyk, editor)). *PLoS Biol* 17: e3000045.

9. Weiss AR, Gillies MJ, Philiastides MG, Apps MA, Whittington MA, FitzGerald JJ, *et al.* (2018): Dorsal Anterior Cingulate Cortices Differentially Lateralize Prediction Errors and Outcome Valence in a Decision-Making Task. *Front Hum Neurosci* 12: 203.
10. Kanai R, Paulus W, Walsh V (2010): Transcranial alternating current stimulation (tACS) modulates cortical excitability as assessed by TMS-induced phosphene thresholds. *Clinical Neurophysiology* 121: 1551–1554.
11. Schutter DJLG (2014): Syncing your brain: electric currents to enhance cognition. *Trends in Cognitive Sciences* 18: 331–333.
12. Kim Y, Lee J-H, Park J-C, Kwon J, Kim H, Seo J, Min B-K (2024): Neuromodulation of inhibitory control using phase-lagged transcranial alternating current stimulation. *J NeuroEngineering Rehabil* 21: 93.
13. Onoda K, Kawagoe T, Zheng H, Yamaguchi S (2017): Theta band transcranial alternating current stimulations modulates network behavior of dorsal anterior cingulate cortex. *Sci Rep* 7: 3607.
14. Guo W, He Y, Zhang W, Sun Y, Wang J, Liu S, Ming D (2023): A novel non-invasive brain stimulation technique: “Temporally interfering electrical stimulation.” *Front Neurosci* 17: 1092539.
15. Mirzakhalili E, Barra B, Capogrosso M, Lempka SF (2020): Biophysics of Temporal Interference Stimulation. *Cell Syst* 11: 557-572.e5.

16. Violante IR, Alania K, Cassarà AM, Neufeld E, Acerbo E, Carron R, *et al.* (2022): *Non-Invasive Temporal Interference Electrical Stimulation of the Human Hippocampus*. Neuroscience. https://doi.org/10.1101/2022.09.14.507625

17. Wessel MJ, Beanato E, Popa T, Windel F, Vassiliadis P, Menoud P, *et al.* (2023): Noninvasive theta-burst stimulation of the human striatum enhances striatal activity and motor skill learning. *Nat Neurosci* 26: 2005–2016.

18. Wang M, Lou K, Liu Z, Wei P, Liu Q (2023): Multi-objective optimization via evolutionary algorithm (MOVEA) for high-definition transcranial electrical stimulation of the human brain. *Neuroimage* 280: 120331.

19. Yaakub SN, White TA, Roberts J, Martin E, Verhagen L, Stagg CJ, *et al.* (2023): Transcranial focused ultrasound-mediated neurochemical and functional connectivity changes in deep cortical regions in humans. *Nat Commun* 14: 5318.

20. Holroyd CB, Coles MGH (2002): The neural basis of human error processing: Reinforcement learning, dopamine, and the error-related negativity. *Psychological Review* 109: 679–709.

21. Walsh MM, Anderson JR (2012): Learning from experience: Event-related potential correlates of reward processing, neural adaptation, and behavioral choice. *Neuroscience & Biobehavioral Reviews* 36: 1870–1884.

22. Foti D, Hajcak G (2009): Depression and reduced sensitivity to non-rewards versus rewards: Evidence from event-related potentials. *Biological Psychology* 81: 1–8.

23. Sambrook TD, Goslin J (2015): A neural reward prediction error revealed by a meta-

analysis of ERPs using great grand averages. *Psychological Bulletin* 141: 213–235.

24. Chase HW, Swainson R, Durham L, Benham L, Cools R (2011): Feedback-related Negativity Codes Prediction Error but Not Behavioral Adjustment during Probabilistic Reversal Learning. *Journal of Cognitive Neuroscience* 23: 936–946.

25. Cohen MX (2008): Neurocomputational mechanisms of reinforcement-guided learning in humans: a review. *Cogn Affect Behav Neurosci* 8: 113–125.

26. Reinhart RMG, Woodman GF (2014): Causal Control of Medial–Frontal Cortex Governs Electrophysiological and Behavioral Indices of Performance Monitoring and Learning. *J Neurosci* 34: 4214–4227.

27. Holroyd CB, Nieuwenhuis S, Yeung N, Nystrom L, Mars RB, Coles MGH, Cohen JD (2004): Dorsal anterior cingulate cortex shows fMRI response to internal and external error signals. *Nat Neurosci* 7: 497–498.

28. Koob GF, Volkow ND (2010): Neurocircuitry of Addiction. *Neuropsychopharmacol* 35: 217–238.

29. Goldstein RZ, Volkow ND (2011): Dysfunction of the prefrontal cortex in addiction: neuroimaging findings and clinical implications. *Nat Rev Neurosci* 12: 652–669.

30. Simon JJ, Skunde M, Wu M, Schnell K, Herpertz SC, Bendszus M, *et al.* (2015): Neural dissociation of food- and money-related reward processing using an abstract incentive delay task. *Social Cognitive and Affective Neuroscience* 10: 1113–1120.

31. Balodis IM, Potenza MN (2015): Anticipatory Reward Processing in Addicted Populations: A Focus on the Monetary Incentive Delay Task. *Biological Psychiatry* 77: 434–444.

32. Grossman N, Bono D, Dedic N, Kodandaramaiah SB, Rudenko A, Suk H-J, *et al.* (2017): Noninvasive Deep Brain Stimulation via Temporally Interfering Electric Fields. *Cell* 169: 1029-1041.e16.

33. Mirzakhalili E, Barra B, Capogrosso M, Lempka SF (2020): Biophysics of Temporal Interference Stimulation. *Cell Systems* 11: 557-572.e5.

34. Baayen RH, Davidson DJ, Bates DM (2008): Mixed-effects modeling with crossed random effects for subjects and items. *Journal of Memory and Language* 59: 390–412.

35. Haber SN, Knutson B (2010): The Reward Circuit: Linking Primate Anatomy and Human Imaging. *Neuropsychopharmacol* 35: 4–26.

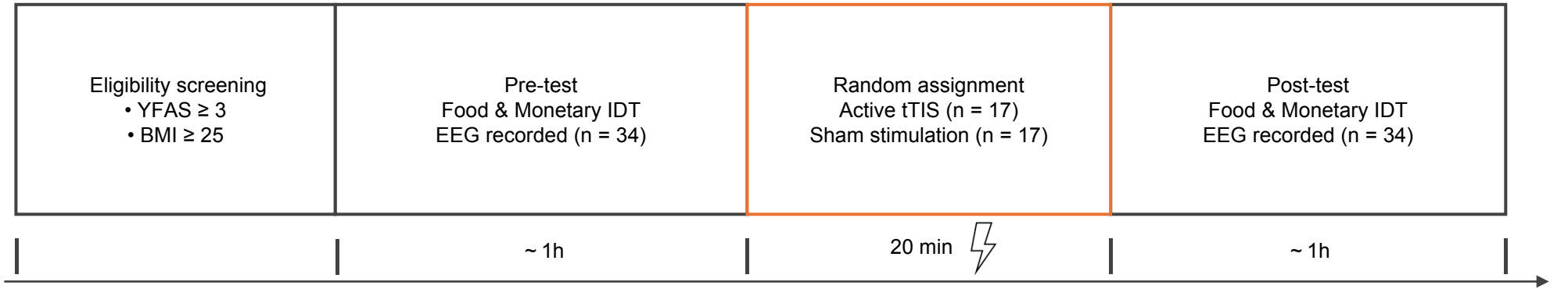
Eligibility screening
• YFAS ≥ 3
• BMI ≥ 25
Pre-test
Food & Monetary IDT
EEG recorded (n = 34)
Random assignment
Active tTIS (n = 17)
Sham stimulation (n = 17)
Post-test
Food & Monetary IDT
EEG recorded (n = 34)
~ 1h
20 min
~ 1h

A: Practice

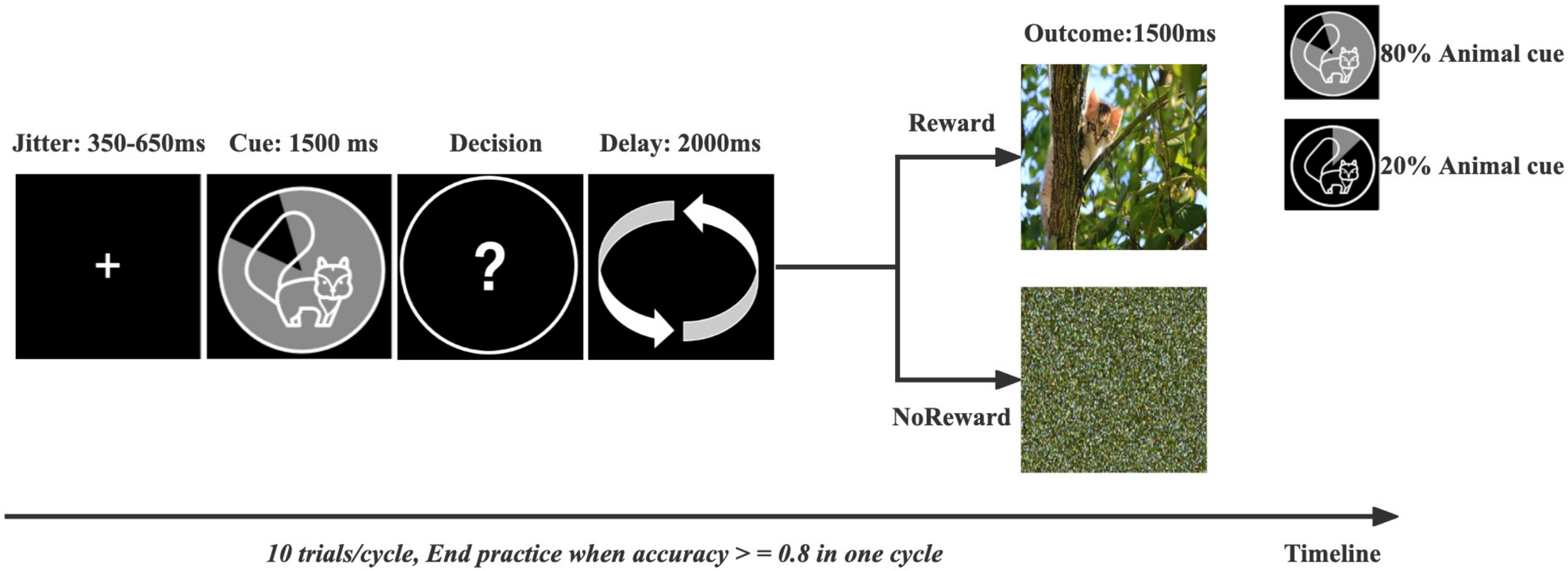

B: Money and Food incentive delay task

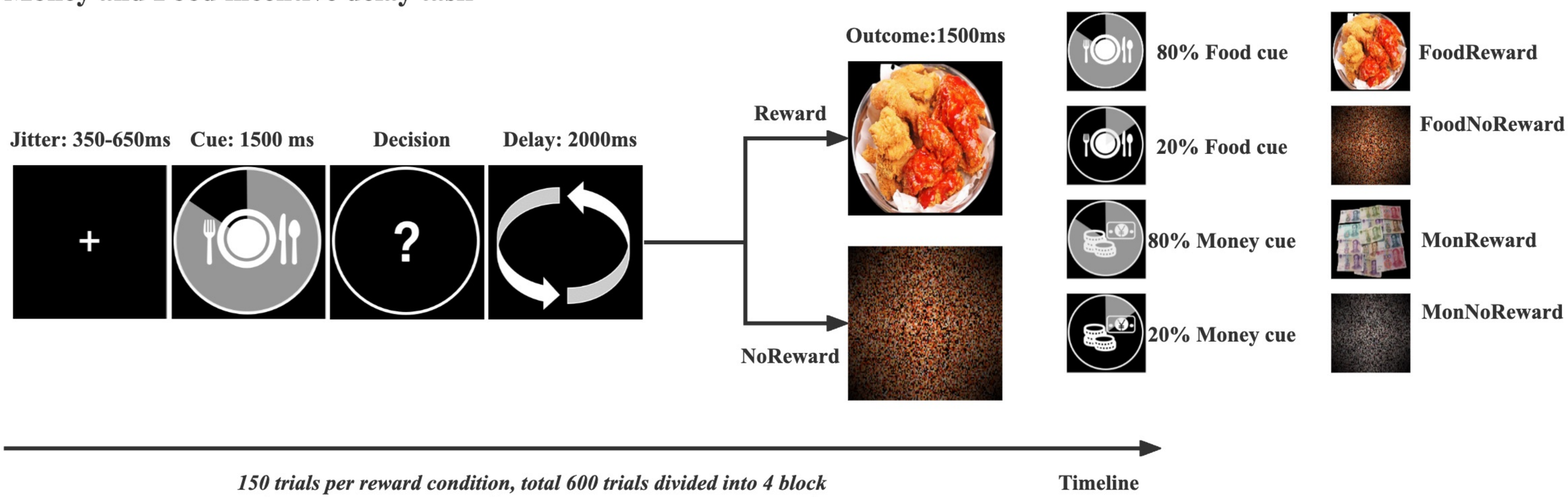

Reward condition	*Outcomes*
FoodReward	*Food picture*
FoodNoReward	*Food scrambled picture*
MonReward	*Monetary picture*
MonNoReward	*Monetary scrambled picture*

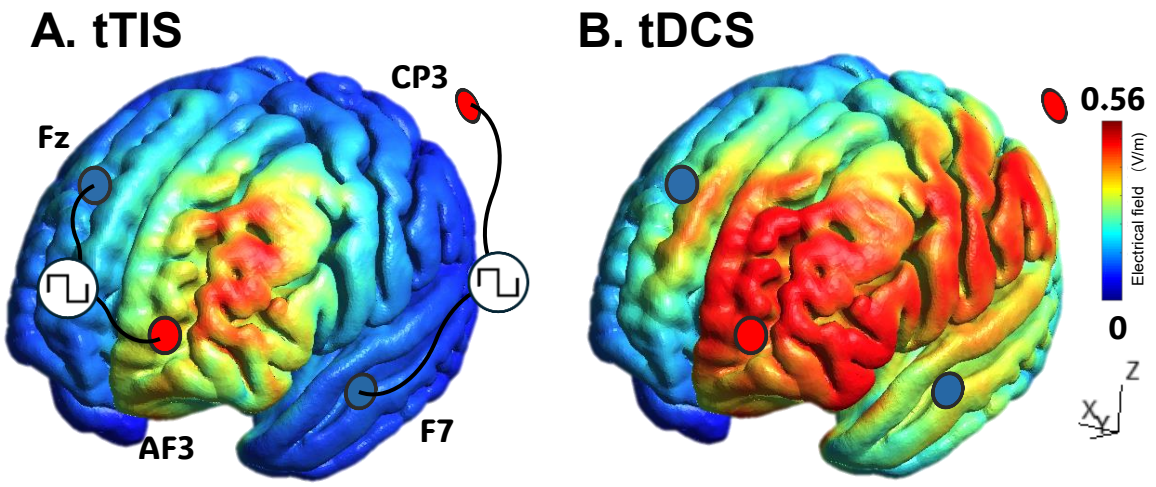
A. tTIS
CP3
Fz
AF3
F7
B. tDCS
0.56
Electrical field (V/m)
0
Z
X
Y

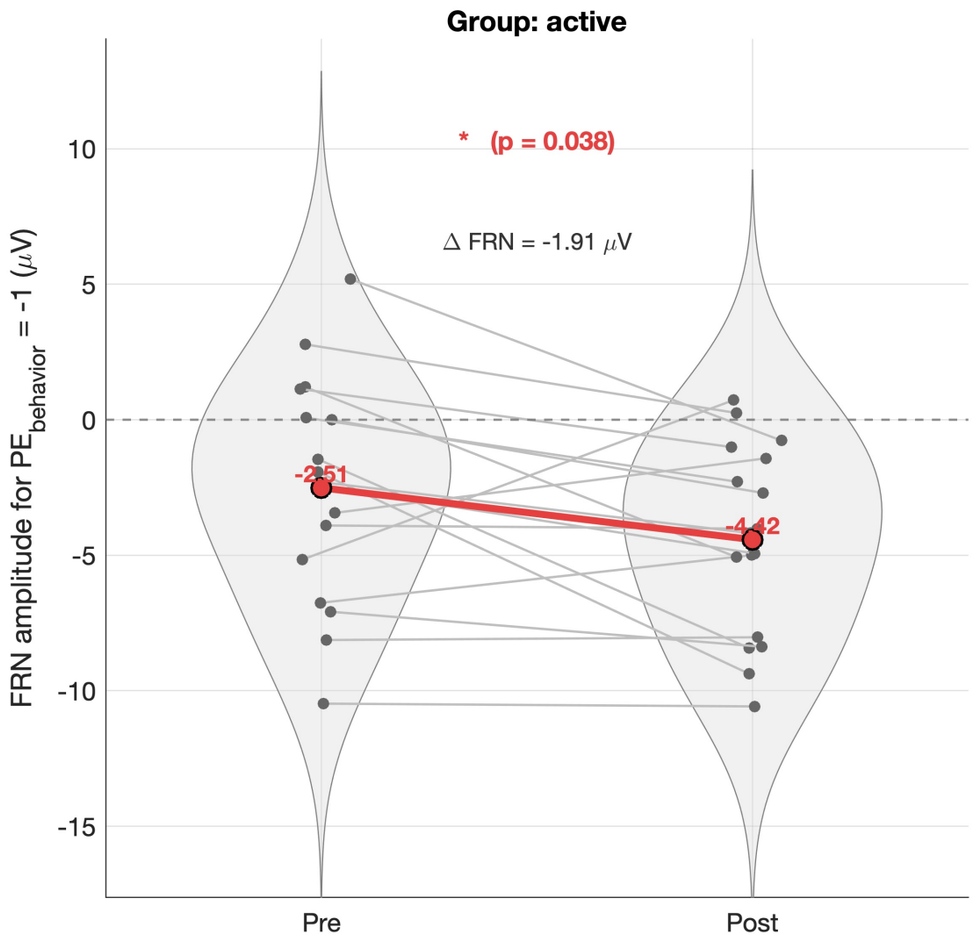
Group: active
* (p = 0.038)
Δ FRN = -1.91 μV
-2.51
-4.42
FRN amplitude for PE behavior = -1 (μV)
10
5
0
-5
-10
-15
Pre
Post

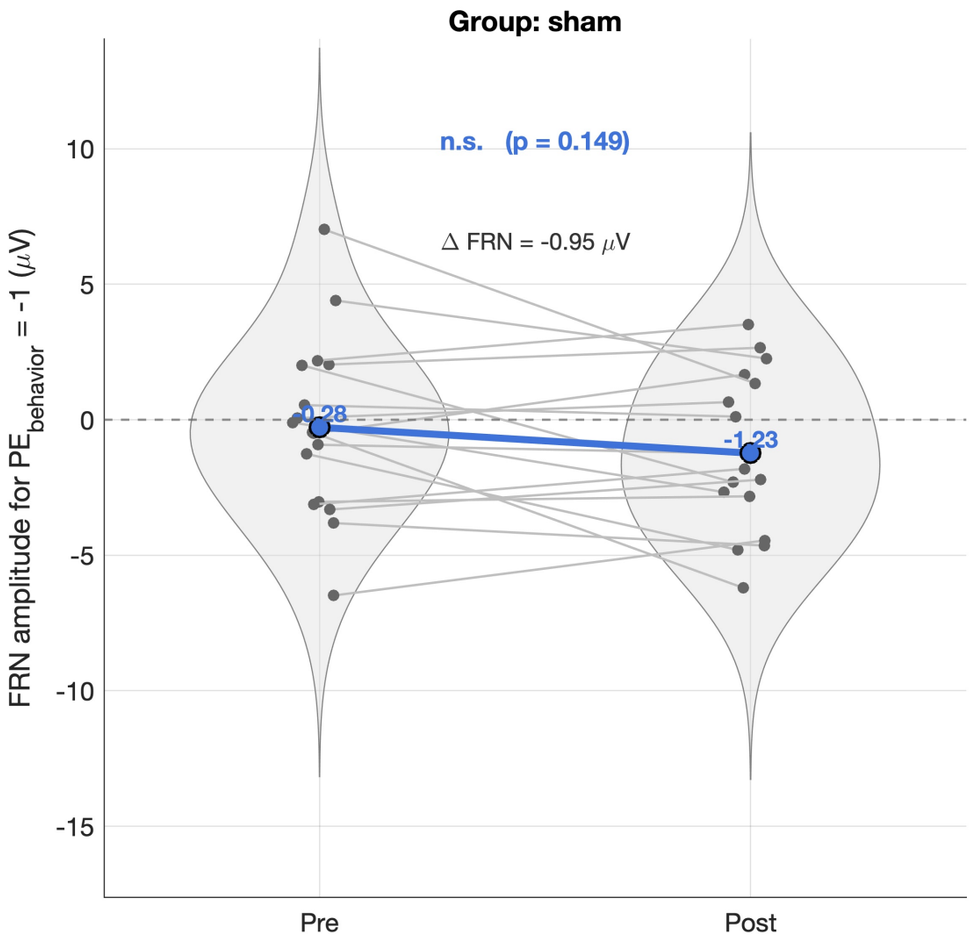
Group: sham
n.s. (p = 0.149)
Δ FRN = -0.95 μV
-0.28
-1.23
FRN amplitude for PE behavior = -1 (μV)
10
5
0
-5
-10
-15
Pre
Post

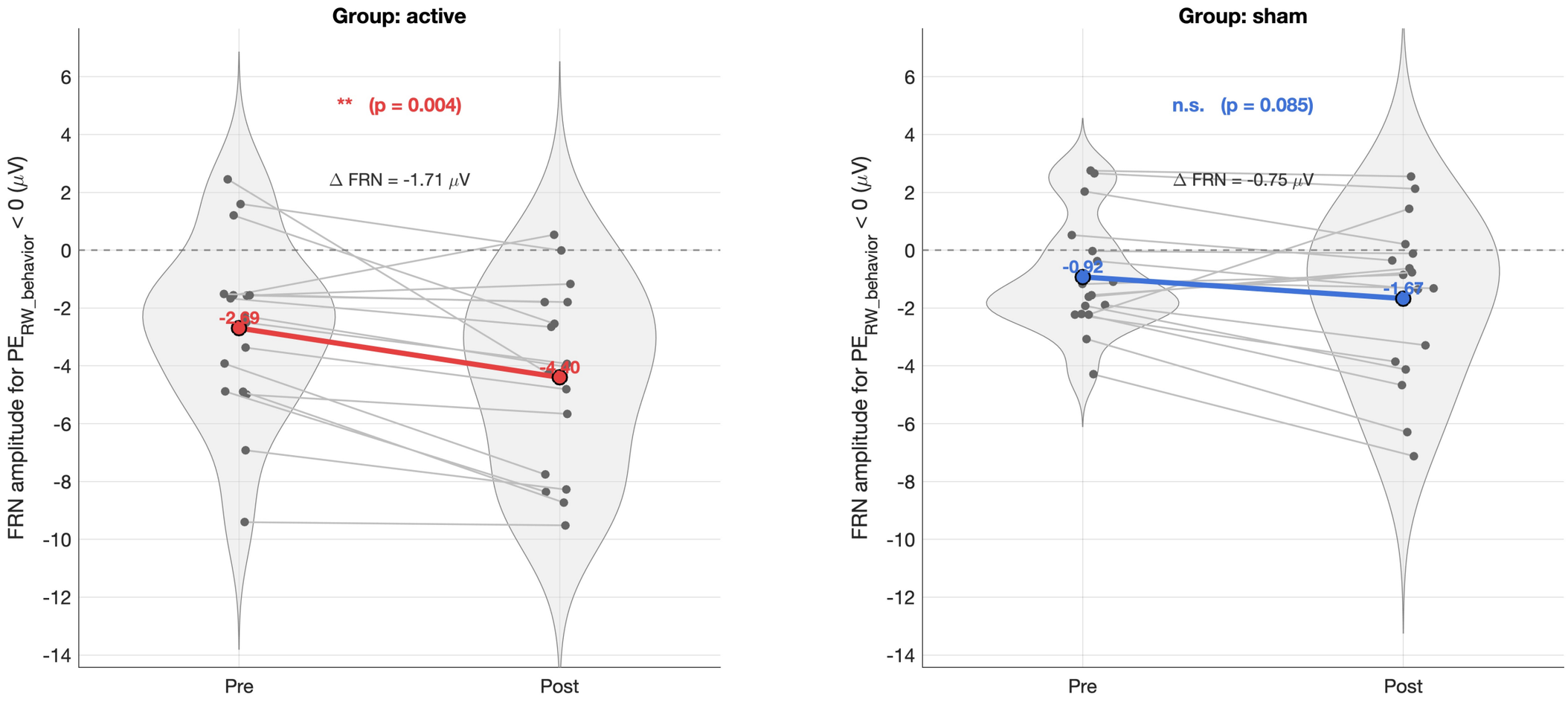
Group: active
** (p = 0.004)
Δ FRN = -1.71 μV
-2.09
-4.00
FRN amplitude for PE_RW_behavior < 0 (μV)
6
4
2
0
-2
-4
-6
-8
-10
-12
-14
Pre
Post
Group: sham
n.s. (p = 0.085)
Δ FRN = -0.75 μV
-0.92
-1.67
FRN amplitude for PE_RW_behavior < 0 (μV)
6
4
2
0
-2
-4
-6
-8
-10
-12
-14
Pre
Post

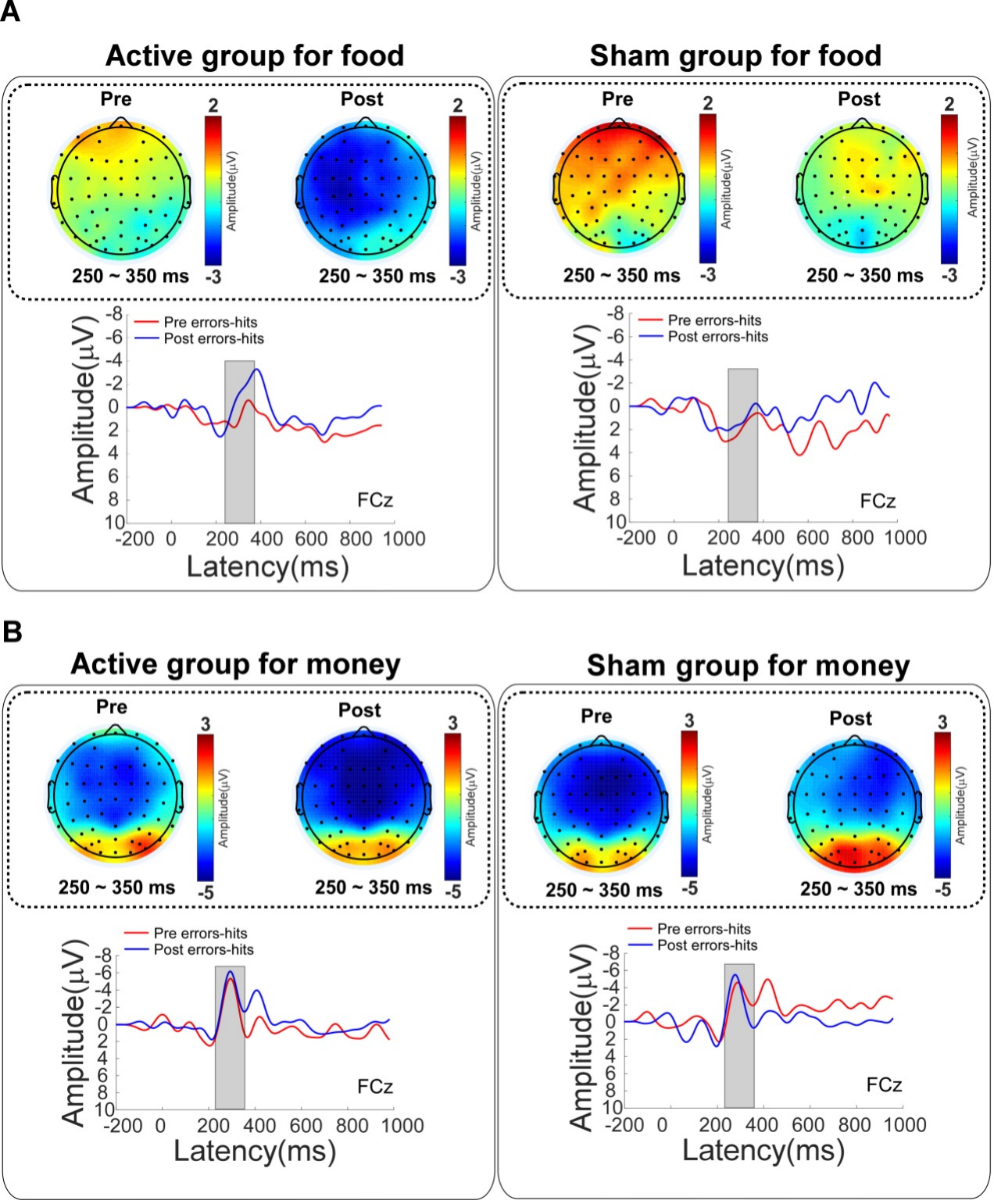
A
Active group for food
Sham group for food
Pre
Post
2
-3
Amplitude(μV)
250 ~ 350 ms
Pre errors-hits
Post errors-hits
FCz
Latency(ms)
B
Active group for money
Sham group for money
3
-5

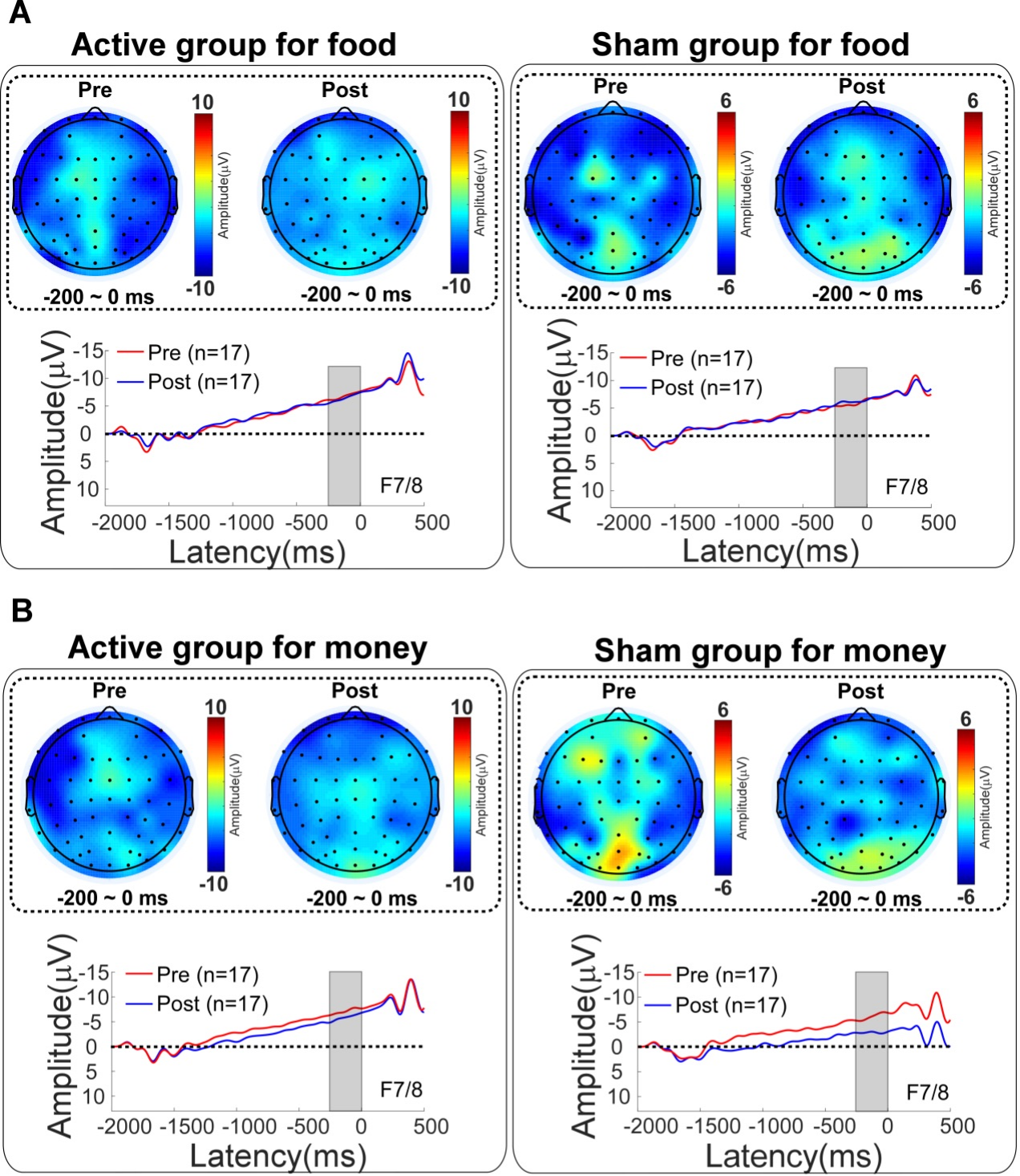
A
Active group for food
Sham group for food
Pre
Post
10
-10
6
-6
Amplitude(μV)
-200 ~ 0 ms
Pre (n=17)
Post (n=17)
F7/8
Amplitude(μV)
Latency(ms)
B
Active group for money
Sham group for money

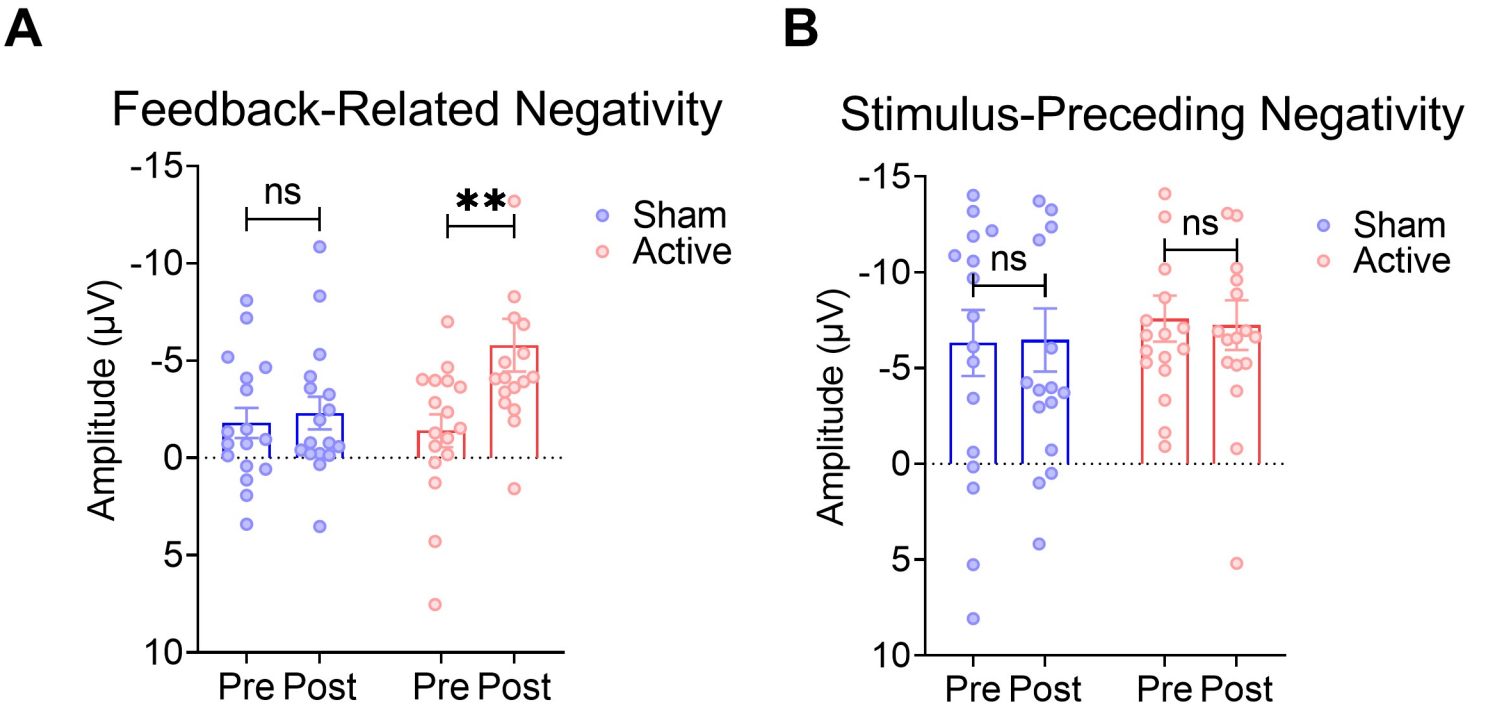
A
Feedback-Related Negativity
Amplitude (μV)
-15
-10
-5
0
5
10
ns
**
Sham
Active
Pre Post
Pre Post
B
Stimulus-Preceding Negativity
Amplitude (μV)
-15
-10
-5
0
5
10
ns
ns
Sham
Active
Pre Post
Pre Post